AIMS Mathematics, 11(5): 14323–14340.
DOI: 10.3934/math.2026588
Received: 09 March 2026
Revised: 28 April 2026
Accepted: 08 May 2026
Published: 20 May 2026

https://www.aimspress.com/journal/Math

Research article

Trajectory tracking control of the hydraulic servo system subject to random impulsive disturbances

Mingzhong Li[1], Yuhao Qi[2], Wei Wang[1], Yongming Li[2], Zhen Fu[1], Qing Liu[1] and Shuai Liu[1,*]

[1] Beijing Tianma Intelligent Control Technology Co., Ltd., Beijing 101399, China
[2] Shandong Energy Group Co., Ltd., Jinan 250101, China

* **Correspondence:** Email: liushuai@tdmarco.com.

Abstract: This paper focuses on analyzing the dynamic model and the stability of the hydraulic servo system, where the random impulsive disturbances are fully considered. To address these issues and achieve the tracking control of the hydraulic support pushing system subject to random impulsive disturbances, we present the mathematical model of the hydraulic support pushing system and define the error variables to complete the design of the controller. Based on the Lyapunov backstepping method, the designed controller can guarantee the error variables converge to zero exponentially and defend random impulsive disturbances effectively, which enhances the robustness of the hydraulic support pushing system. Finally, the validity of the proposed control method is verified by two simulation examples.

Keywords: hydraulic servo system; random impulsive disturbances; trajectory tracking control; Lyapunov backstepping method; exponential stability
Mathematics Subject Classification: Primary: 93DXX; Secondary: 93C05, 93D15, 93D23

1. Introduction

Recently, in response to the growing importance of coal mine safety and the development of coal mining technologies, traditional mechanized backfilling and automated control systems face challenges due to the complex and variable nature of the backfilling process, which makes it difficult to meet stringent requirements and adapt to diverse environments [1–5]. As a main equipment for coal mine filling operations, the hydraulic support pushing system plays a crucial role in enhancing filling efficiency, ensuring a stable filling body, and managing gob safety [6–12]. Nowadays, although there have been some advanced methods about control strategy, such as sliding mode control [13, 14], fault-tolerant control [15], H_∞ control [16, 17], and observer-based control [18], how to control the hydraulic servo system more effectively and accurately is still an attractive topic.

At present, the research on the control of hydraulic support pushing systems is increasingly interdisciplinary. Many scholars have made remarkable progress in system modeling, control strategy optimization, experimental verification, and other aspects, such as [18–25]. In [18], a disturbance observer-based fixed-time event-triggered controller was proposed for an electro-hydraulic system, where input saturation was fully considered. Note that the co-simulation technology for mining machinery has been studied and applied in [19]. In order to satisfy the need of a hydraulic support model test, the data collecting and processing system of the hydraulic support model test was established in [20]. What's more, a multi-segment pushing curve synchronous control model was proposed in [21]. The pushing curve segmentation and segmented curve classification were described in it. [22] proposed a segmented control strategy, which combined bang-bang control and predictive control to achieve the millimeter-level position control of the hydraulic support pushing system. [23] presented a feed-forward compensation decoupling method for the displacement-force dynamic coupling problem caused by the coupling of hydraulic cylinders and pumping stations. It adopted adaptive sliding mode control to suppress system jitter and external disturbances. Moreover, [24] proposed an AdaBoost-backpropagation method to evaluate the internal leakage, which improved the hydraulic support accuracy and safety. Subsequently, [25] presented a novel prescribed performance fault-tolerant control method for electro-hydraulic servo systems. Although external disturbances and unknown nonlinearities were discussed in [25], the discontinuous disturbance was excluded from their topic.

On the other hand, from the perspective of engineering, impulsive disturbance is a kind of discontinuous disturbance that can lead the system to suddenly change in a moment; see [26–34]. This type of disturbance is highly destructive, requiring only a single interruption to crash the entire system dynamics. Generally speaking, impulsive disturbances occur randomly, which means that the disturbance sequences are uncertain. This disturbance form is more challenging for dynamic systems. In [32], target tracking of omnidirectional mobile robots subject to impulsive disturbances was studied, where impulsive disturbances occur in the form of data deception. [33] was concerned with the stability problem for a class of Lipschitz-type nonlinear systems in networked environments, which suffer from random and impulsive disturbances. In [34], a backstepping-based impulsive correction control was proposed to solve the position control problem of the electro-hydraulic servo system, where the input-to-state stability of the error system is researched. Additionally, in the hydraulic support pushing system and even the entire field of mine and factory automation, impulsive disturbance is an important factor, which influences the reliability and safety of the equipment. It always stems from transient processes within the system, such as the operation of solenoid valves, and externally, which threatens the electronic control system through conduction and radiation pathways. Moreover, its harm can range from abnormal data and communication interruption to equipment maloperation or even safety accidents in severe cases. Synthesizing the above analysis, the existing results on the control of hydraulic support pushing systems involving random impulsive disturbances are still limited, and it is necessary to design a controller to defend random impulsive disturbances. In fact, to address the above problems, some difficulties and challenges will be encountered: One is how to give a mathematical model for the hydraulic support pushing mechanism. Another is how to restrain the negative effects of impulsive disturbances on the hydraulic support pushing system during the process of designing the controller.

Through the above analysis, we consider the trajectory tracking control problem of hydraulic

support pushing systems subject to random impulsive disturbances and use the Lyapunov backstepping method to complete the design of the controller. The main contributions of this paper are described as follows: One is that a mathematical model of the hydraulic support pushing system is simplified and given, and random impulsive disturbances are considered in this paper. Another is that the relationship between control law, random impulsive sequences, and the intensity of impulsive disturbances is established, which ensures the stability and enhances robustness of the hydraulic pushing system under the input of our controller.

The remaining part of the paper is described as follows. In Section 2, the mathematical model of the hydraulic support pushing system and its error system subject to random impulsive disturbances is given. Some essential knowledge and a necessary lemma are introduced. Next, the Lyapunov backstepping method is utilized to complete the design of the controller and provide the stability analysis in Section 3. We resort to the simulation results to verify the availability of the controller design in Section 4. In Section 5, we summarize the whole paper and present the conclusion of this paper.

2. Problem formulation

2.1. Notations

The symbols $\mathbb{R}$ and $\mathbb{Z}$ are represented as the set of real numbers and the set of integers. $\mathbb{R}^n$ is the n-dimensional real space equipped with the Euclidean norm $|\cdot|$, $\mathbb{R}_+ \doteq \{a \in \mathbb{R} : a \geq 0\}$, and $\mathbb{Z}_+ \doteq \{a \in \mathbb{Z} : a > 0\}$. $(\Omega, \mathcal{F}, \mathcal{P})$ represents a complete probability space with a natural filtration $\{\mathcal{F}_t\}_{t\geq 0}$ satisfying the general conditions, i.e., $\{\mathcal{F}_t\}_{t\geq 0}$ is monotonic increasing and right-continuous and contains all of the $\mathcal{P}$-null sets. $I(\cdot)$ stands for the indicator function. $\mathbb{E}(\cdot)$ denotes the mathematical expectation operator. D^+ denotes the right-hand upper Dini derivative.

2.2. Characteristics of pushing mechanism

The position control of the straightness of the working surface is essentially a multi-body dynamics coupling problem, and its core control mechanism stems from the interaction between the dynamic characteristics of the hydraulic support pushing system and the structural design. The hydraulic support pushing system of the fully mechanized mining face is shown in Figures 1 and 2. The core of the position control of the hydraulic support pushing system lies in precisely controlling the displacement y of the piston rod. This displacement is driven by the hydraulic pressure acting on the piston, and the hydraulic pressure depends on the pressures P_1 and P_2 in the rodless and rod-bearing chambers of the hydraulic cylinder. The variation of pressure is controlled by the flow rates Q_1 and Q_2 flowing into and out of the rodless and rod-bearing chambers of the hydraulic cylinder, respectively. The flow rate is directly determined by the displacement y_v of the valve core and the pressure difference at the valve port. Therefore, establishing an accurate valve-controlled hydraulic cylinder system model is the foundation of position control. The structure of hydraulic support pushing mechanism is shown in Figure 3.

The flow equation of the valve is:

$$Q_L = K_q y_v - K_c P_L, \tag{2.1}$$

where Q_L represents load traffic; K_q is the flow gain; and K_c is the flow-pressure coefficient. P_L stands for load pressure. When the piston moves, the flow rates Q_1 in the rodless cavity and Q_2 in the rod-bearing cavity are

$$\begin{cases} Q_1 = A_1 \frac{dy}{dt}, \\ Q_2 = A_2 \frac{dy}{dt}, \end{cases} \tag{2.2}$$

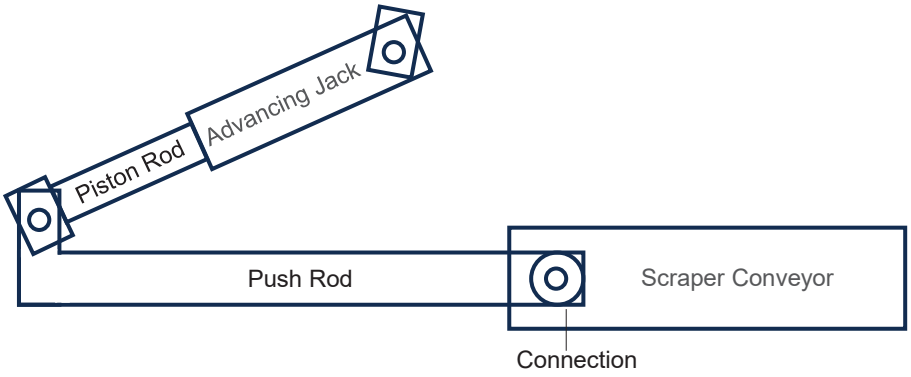

Figure 1. Schematic diagram of the connection of the hydraulic support pushing system.

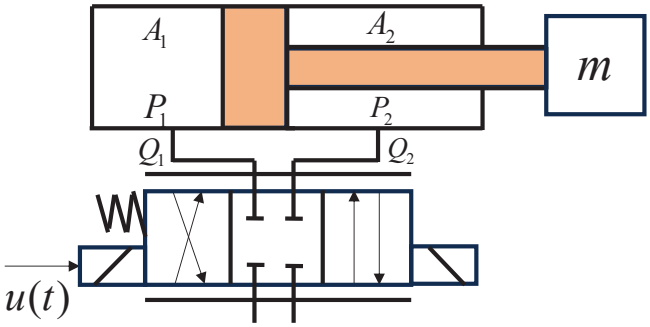

Figure 2. Working principle of the hydraulic cylinder.

Figure 3. Structure of the hydraulic support pushing mechanism.

where t denotes the time. The effective area ratio of the rodless cavity A_1 and the rod-bearing cavity A_2 is $N = \frac{A_1}{A_2}$. To eliminate the influence of the area ratio N, the flow rates of the two cavities are weighted and combined:

$$Q_L = \frac{Q_1 + NQ_2}{1 + N^2}. \tag{2.3}$$

The change in flow rate caused by the compressibility of the oil is

$$\Delta Q = \frac{V_t}{2\beta_e}\frac{dP_L}{dt}, \tag{2.4}$$

where V_t represents the total volume of the hydraulic cylinder. β_e is the equivalent elastic modulus of the oil. To compare the flow variation ΔQ of the two chambers, we perform normalization with respect to the area ratio N:

$$\Delta Q = \frac{V_t}{2\beta_e(1 + N^2)}\frac{dP_L}{dt}. \tag{2.5}$$

The external leakage flow rate C_{te} is directly proportional to the load pressure P_L, and the internal leakage flow rate C_{teo} is directly proportional to the fuel supply pressure P_S. Comprehensively considering the influence of piston movement, the flow variation of oil compressibility and, leakage effect, the flow equation of the hydraulic cylinder is derived based on Eq (2.6):

$$Q_L = A_1\frac{dy}{dt} + \frac{V_t}{2(1 + N^2)\beta_e}\frac{dP_L}{dt} + C_{te}P_L + C_{teo}P_S. \tag{2.6}$$

The force balance equation of the hydraulic rod is

$$A_1P_1 - A_2P_2 = M\ddot{y} + B_c\dot{y} + My + F_L, \tag{2.7}$$

where M represents the elastic stiffness of the load and B_c is the viscous damping coefficient of the piston and the load. F_L stands for load force. By combining Eqs (2.1), (2.6), and (2.7) and performing the Laplace transform and derivation simplification, the system transfer function can be obtained:

$$\frac{Y}{Y_{\mathrm{v}}} = \frac{\frac{K_{\mathrm{q}}A_1}{K_{\mathrm{c}}}\left(\frac{s^2}{\omega_{\mathrm{h}}^2} + \frac{2\xi_{\mathrm{m}}}{\omega_{\mathrm{h}}}s + 1\right)}{\left(\frac{s}{\omega_{\mathrm{r}}} + 1\right)\left(\frac{s^2}{\omega_0^2} + \frac{2\xi_0}{\omega_0}s + 1\right)}, \tag{2.8}$$

where Y represents the displacement of the piston rod after Laplace transform and Y_v represents the displacement of the valve core after Laplace transform. s is a complex variable; ω_h represents the mechanical natural frequency. ξ_m is the mechanical damping coefficient; ω_r represents the turning frequency; and K_{ce} represents the total flow pressure coefficient. ω_0 is the natural frequency; ξ_0 represents the hydraulic and mechanical damping coefficients; and M_h represents the stiffness of the hydraulic spring, where

$$\xi_m = \frac{B_c}{2\sqrt{mk}},\ \omega_r = \frac{MK_{ce}}{A_1^2},$$
$$\omega_0 = A_1\sqrt{1 + \frac{M}{M_h}}\frac{2(1 + N^2)\beta_e}{mV_t},$$
$$\xi_0 = \frac{K_{ce}}{1 + M/M_h}\sqrt{\frac{(1 + N^2)\beta_e m}{2V_t}} + \frac{B_c}{2A_1}\frac{V_t}{2(1 + N^2)\beta_e m}.$$

2.3. The error description of the hydraulic support pushing system

For this nonlinear control system, it needs to be converted into a state equation for consideration. Based on the above discussion and taking the state variable $[x_1, x_2, x_3]^T = [y, \dot{y}, \ddot{y}]^T$, the actual system can be obtained as

$$\begin{cases} \dot{x}_1(t) = x_2(t), \\ \dot{x}_2(t) = x_3(t), \\ \dot{x}_3(t) = f_1 x_2(t) + f_2 x_3(t) + g u(t), \\ y = x_1, \end{cases} \tag{2.9}$$

where $f_1 = \omega_h(1 + \frac{K_q k}{2A_1 - A_2})$, $f_2 = \omega_h \xi_0$; g is the gain coefficient of the control voltage, where $g = \frac{K_q \omega_h^2}{2A_1 - A_2}$; and $u(t)$ is the control voltage.

In this paper, our objective is to enable the actual hydraulic support pushing system to track the desired system under the control input $u(t)$, where the desired system is given by

$$\begin{cases} \dot{x}_{1d}(t) = x_{2d}(t), \\ \dot{x}_{2d}(t) = x_{3d}(t), \\ \dot{x}_{3d}(t) = f_1 x_{2d}(t) + f_2 x_{3d}(t), \\ y_d = x_{1d}. \end{cases} \tag{2.10}$$

By subtracting systems (2.9) and (2.10), we can obtain the error system of the hydraulic support pushing system:

$$\begin{cases} \dot{e}_1(t) = e_2(t), \\ \dot{e}_2(t) = e_3(t), \\ \dot{e}_3(t) = f_1 e_2(t) + f_2 e_3(t) + g u(t). \end{cases} \tag{2.11}$$

In the actual operation of the hydraulic support pushing system, it is disturbed frequently by instantaneous external factors, and the sequence of the disturbances is often random. Therefore, impulse jumps are introduced to characterize stochastic impulsive disturbances from the external factors such as sudden forces and data deception attacks from sensors. Consider the mathematical model of random impulsive disturbances:

$$e_i(t) = \beta e_i(t^-), \ i = 1, 2, 3, \ t = t_k, \tag{2.12}$$

where β is the intensity of impulsive disturbances. When β is slightly larger than 1, it corresponds to mild impulsive effects, such as small pressure fluctuations, weak valve-switching transients, or minor sensor signal jumps. A larger β indicates stronger instantaneous disturbances, such as abrupt load impacts, significant hydraulic pressure shocks, or larger measurement and communication jumps, which may cause more obvious deviations in displacement, velocity, or acceleration errors. The time sequence of stochastic impulsive disturbances is denoted by $\mathcal{S} \triangleq \{t_k\}_{k=0}^{\infty}$ with $t_0 = 0$ satisfying $0 < t_1 < t_2 < \cdots < t_n \to +\infty$ as $n \to +\infty$. Furthermore, let $t_k = \sum_{i=1}^{k} \tau_i$, and if $\{\tau_i\}_{i=1}^{\infty}$ is a sequence of independent exponentially distributed random variables with a parameter $\lambda > 0$, then we represent

such kind of impulse time sequences as $\mathcal{S}_\lambda$. Let $N(t, s)$ indicate the number of impulse instants on the interval $(s, t]$ with $0 \leq s < t$.

Remark 1. The impulsive form $e_i(t) = \beta e_i(t^-)$ is adopted for the following specific reasons. First, in many industrial networked control systems, the sensor communication link may suffer from proportional deception attacks or electromagnetic interference that scales the true measurement by a factor β before it reaches the controller. Since the controller operates on the corrupted signal, the resulting error dynamics experience a multiplicative jump even if the physical plant state does not jump. Second, hydraulic pressure surges induced by abrupt valve closure can produce an instantaneous acceleration increment that is approximately proportional to the current piston velocity. Consequently, a larger pre-impulse velocity leads to a proportionally larger jump in the position or velocity error. In both scenarios, the intensity of the jump depends on the current deviation, which is faithfully captured by the multiplicative model. Therefore, we utilize the form (2.12) to represent these actual situations, which is not only conducive to theoretical analysis but also conforms to the actual situation.

In the following, the error system of the hydraulic support pushing mechanism subject to random impulsive disturbances is given by

$$\begin{cases} \dot{e}_1(t) = e_2(t), \ t \neq t_k, \\ \dot{e}_2(t) = e_3(t), \ t \neq t_k, \\ \dot{e}_3(t) = f_1 e_2(t) + f_2 e_3(t) + gu(t), \ t \neq t_k, \\ e_i(t) = \beta e_i(t^-), \ i = 1, 2, 3, \ t = t_k, \end{cases} \tag{2.13}$$

where $k \in \mathbb{Z}_+$, $e(t) = [e_1(t), e_2(t), e_3(t)]^T \in \mathbb{R}^3$ is the system state and the initial condition $e_0 = [e_1(0), e_2(0), e_3(0)]^T \in \mathbb{R}^3$. In this paper, we suppose that the solutions of system (2.13) are right continuous and exist uniquely.

Lemma 1. Let $N(t) \triangleq \sum_{k=0}^{\infty} kI(t_k \leq t \leq t_{k+1})$. It can be inferred that $N(t)$ represents the number of impulses occurring on the interval $(0, t]$. The stochastic process $\{N(t), t \geq 0\}$ is a Poisson process with parameter $\lambda \geq 0$ and for any $0 = t_0 \leq s \leq t$. The increment $N(t) - N(s)$ has a Poisson distribution with the parameter $\lambda(t - s)$. Let $N(s, t) = N(t) - N(s)$, then

$$\mathbb{P}\{N(s, t) = k\} = e^{-\lambda(t-s)} \frac{[\lambda(t - s)]^k}{k!}, \ k = 0, 1, 2, ...$$

Definition 1. For a given impulse time sequence $\{t_k\} \in \mathcal{S}$, we denote $e(t) = e(t, 0, x_0, \{t_k\})$ as the solution of system (2.13) starting from $(0, e_0)$ and subject to impulse actions at time sequence $\{t_k\}$. Then system (2.13) is said to be p-th moment exponentially stable (p-ES) with Ξ if there are two scalars $\lambda > 0$ and $\mathcal{M} \geq 1$ such that

$$\mathbb{E}|e(t)|^p \leq \mathcal{M} \cdot |e_0|^p \exp(-\lambda t), \ \forall t \geq 0 \tag{2.14}$$

for any initial value $e_0 \in \Xi$. Specially, if (2.14) holds for every sequence $\{t_k\} \in \mathcal{S}$, with two positive scalars λ and $\mathcal{M}$ independent of the choice of $\{t_k\}$, then system (2.13) is said to be uniformly p-ES with Ξ over $\mathcal{S}$.

3. Main results

In this section, we design the controller through Lyapunov backstepping to realize the tracking control to reference signal and defend against the random impulsive disturbances. The control frame of the hydraulic support pushing system is shown as Figure 4.

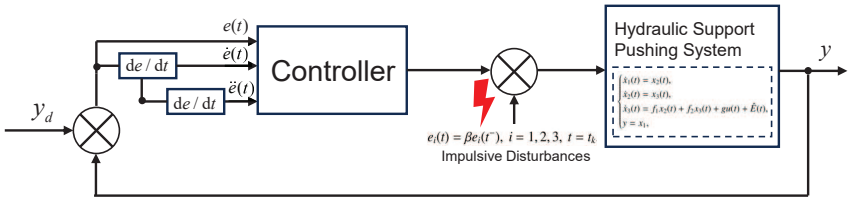

Figure 4. Control frame for the hydraulic support pushing system.

Theorem 1. Error system (2.13) is uniformly 2-*ES* over the class S_λ with $\beta > 1$ by the following control input:

$$u(t) = \frac{1}{g}\left[-(C^3 + 2C)e_1 - (f_1 + 3C^2 + 2)e_2 - (f_2 + 3C)e_3\right], \tag{3.1}$$

where C is a constant satisfying $C > 0.5\lambda(\beta^2 - 1)$.

Proof. Let $e(t) = e(t, 0, e_0, \{t_k\})$ be the solution of system (2.13) through initial state $(0, e_0)$, where $e_0 \in \mathbb{R}^3$ and $\{t_k\} \in \mathcal{S}_\lambda$. For convenience, we denote $V(t) \triangleq V(t, e(t))$ and $V_0 \triangleq V(0, e_0)$. In the following, we utilize the Lyapunov backstepping method to guarantee the exponential stability of system (2.13). Assume that the virtual control variables

$$\begin{cases} z_1 = e_1(t), \\ z_2 = e_2 - \varphi_1(e_1), \\ z_3 = e_3 - \varphi_1(e_1, e_2). \end{cases} \tag{3.2}$$

When $t \neq t_k$, by designing the Lyapunov function as $V_1 = \frac{1}{2}z_1^2$, its time derivative along (2.13) yields

$$D^+V_1(t) = z_1\dot{e}_1 = z_1e_2 = z_1(z_2 + \varphi_1(e_1)). \tag{3.3}$$

Along with (3.3), auxiliary control variable $\varphi_1(e_1)$ can be calculated by

$$\varphi_1(e_1) = -Cz_1, \tag{3.4}$$

where $C > 0$ is a constant. Substituting the designed upper control signal (3.4) into (3.3), the time derivative can be expressed as

$$D^+V_1(t) = -Cz_1^2 + z_1z_2. \tag{3.5}$$

In the following, we choose the Lyapunov function as $V_2 = V_1 + \frac{1}{2}z_2^2$. The time derivative along system (2.13) can be obtained as

$$D^+V_2(t) = -Cz_1^2 + z_1z_2 + z_2\dot{z}_2$$

$$
\begin{aligned}
&= -Cz_1^2 + z_1z_2 + z_2(\dot{e}_2 - \dot{\varphi}_1(e_1)) \\
&= -Cz_1^2 + z_1z_2 + z_2(e_3 - \dot{\varphi}_1(e_1)) \\
&= -Cz_1^2 + z_1z_2 + z_2(z_3 + \varphi_2(e_1, e_2) - \dot{\varphi}_1(e_1)).
\end{aligned} \tag{3.6}
$$

Similarly, auxiliary control variable $\varphi_2(e_1, e_2)$ can be calculated as

$$
\varphi_2(e_1, e_2) = \dot{\varphi}_1(e_1) - Cz_2 - z_1. \tag{3.7}
$$

Therefore, the time derivative of (2.13) is given by

$$
D^+V_2(t) = -Cz_1^2 - Cz_2^2 + z_2z_3. \tag{3.8}
$$

Finally, choosing the Lyapunov function as $V(t) = V_2 + \frac{1}{2}z_3^2$, its time derivative along system (2.13) is

$$
\begin{aligned}
D^+V(t) &= -Cz_1^2 - Cz_2^2 + z_2z_3 + z_3\dot{z}_3 \\
&= -Cz_1^2 - Cz_2^2 + z_2z_3 + z_3(\dot{e}_3 - \dot{\varphi}_2(e_1, e_2)) \\
&= -Cz_1^2 - Cz_2^2 + z_2z_3 + z_3(f_1e_2 + f_2e_3 + gu(t) - \dot{\varphi}_2(e_1, e_2)).
\end{aligned} \tag{3.9}
$$

Then, substituting the designed control law (3.1), we can get the time derivative of system (2.13):

$$
D^+V(t) = -Cz_1^2 - Cz_2^2 - Cz_3^2 = -2CV(t). \tag{3.10}
$$

It then follows from (3.9) and (3.10) that

$$
V(t) = V(t_k)e^{-2C(t-t_k)},\ \forall t \in [t_k, t_{k+1}),\ k \in \mathbb{Z}_+. \tag{3.11}
$$

In view of (3.11), when the stochastic impulsive disturbances are introduced, it can be derived that

$$
V(t) = \beta^{2N(t,0)}V_0e^{-2Ct},\ \forall t \geq 0. \tag{3.12}
$$

By the property of mathematical expectation and taking the mathematical expectation on both sides of (3.12), it yields that

$$
\begin{aligned}
\mathbb{E}V(t) &= \mathbb{E}\left[\sum_{k=0}^{\infty} V(t) \cdot I(N(t,0) = k)\right] \\
&= V_0e^{-2Ct}\sum_{k=0}^{\infty}\mathbb{E}\left[\beta^{2N(t,0)} \cdot I(N(t,0) = k)\right] \\
&= V_0e^{-2Ct}\sum_{k=0}^{\infty}\mathbb{E}\left[\beta^{2N(t,0)}|N(t,0) = k\right] \cdot \mathbb{P}\{N(t,0) = k\}.
\end{aligned} \tag{3.13}
$$

It then follows from Lemma 2.3 and (3.13) that

$$
\begin{aligned}
\mathbb{E}V(t) &= V_0e^{-2Ct}\sum_{k=0}^{\infty}\beta^{2k}e^{-\lambda t}\frac{(\lambda t)^k}{k!} \\
&= V_0e^{(\beta^2\lambda - \lambda - 2C)t},\ \forall t \geq 0,
\end{aligned} \tag{3.14}
$$

which implies that

$$\mathbb{E}|e(t)|^2 \leq 2|e_0|^2 e^{(\beta^2\lambda-\lambda-2C)t}, \ \forall t \geq 0, \tag{3.15}$$

where $\beta^2\lambda - \lambda - 2C < 0$. Hence, system (2.13) is uniformly 2-ES over the class $\mathcal{S}_\lambda$ by control law (3.1). The proof is completed.

Remark 2. Note that [23] proposed a sliding mode strategy to enhance path tracking control effect. However, the control strategy presented in [23] cannot resist the impulsive disturbance. Compared with the controllers proposed in [23], this paper develops a kind of novel controller, in which the negative effects of stochastic impulsive disturbances are fully considered. By establishing the relationship among continuous control laws, stochastic impulsive sequences, and impulsive disturbance intensity, our control gain in controllers can be artificially adjusted to restrain the negative effects of stochastic impulsive disturbance attacks. It demonstrates the robustness of proposed controllers against impulsive disturbances.

Remark 3. In implementation, C can be selected by first estimating or specifying the admissible maximum disturbance intensity $\bar{\beta}$ and maximum occurrence rate $\bar{\lambda}$, and then choosing $C > 0.5\bar{\lambda}(\bar{\beta}^2 - 1)$ with a proper safety margin. Theoretically speaking, a larger C improves convergence speed and disturbance rejection; however, it may also increase control pressure and actuator activity. Therefore, C should be chosen as a moderate value satisfying the theoretical lower bound while avoiding unnecessarily aggressive control action.

4. Simulation

In this section, we take a class of hydraulic support pushing systems as an example. Based on the mathematical model of the hydraulic support pushing system (2.9) and the designed controller (3.1), a simulation model is established in Matlab. Some simulation parameters of the hydraulic support pushing system are presented in Table 1.

Table 1. Parameters of the hydraulic support pushing system in simulation.

Parameter	Meaning	Value
β_e	Elastic modulus of the oil.	700
A_1	Rodless cavity area.	0.0154
A_2	Rod-bearing cavity area.	0.0083
P_s	Fuel supply pressure.	1.6×10^7
V_t	Total volume of the hydraulic cylinder.	0.1×10^{-3}
M	Elastic stiffness of the load.	40000
C_{te}	External leakage flow rate.	4×10^{-11}
B_c	Viscous damping coefficient of the piston and the load.	800

In the first simulation, a step signal with an amplitude of 0.7 m is input into the hydraulic support pushing system (2.10). Note that our objective is to track this step signal subject to random impulsive disturbances. Assume that the intensity of the random impulsive disturbances is $\beta = 1.7$ and the frequency of the random impulsive disturbances is $\lambda = 2$. In the simulation, choose initial values as $[x_{1d}(0), x_{2d}(0), x_{3d}(0)]^T = [0, 2, 1]^T$ and $[x_1(0), x_2(0), x_3(0)]^T = [0.3, 1.7, 0.8]^T$. Then, it can be observed that if we use controller (3.1) with control gain $C = 1$, then the actual displacement $y_{1d}(t) = x_{1d}(t)$ is unable to track the desired step signal under the disturbances of random impulses, as shown in Figure 5. On the other hand, we utilize controller (3.1) with gain $C = 2$ as the system controller, which satisfies the conditions in Theorem 1. Then, the error system converges to 0 under the random impulsive disturbances, as shown in Figure 6. The actual output displacement can track the desired output displacement quickly, as shown in Figure 7.

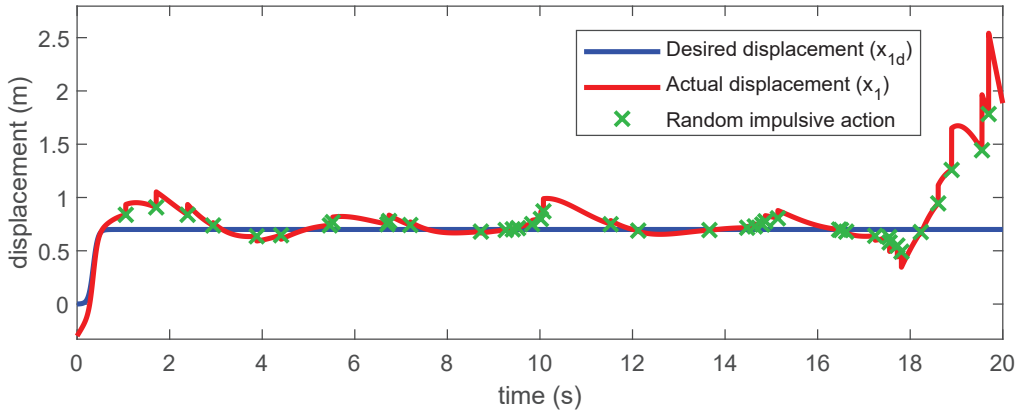

Figure 5. Comparison between the desired displacement and the actual displacement of the step signal with $C = 1$.

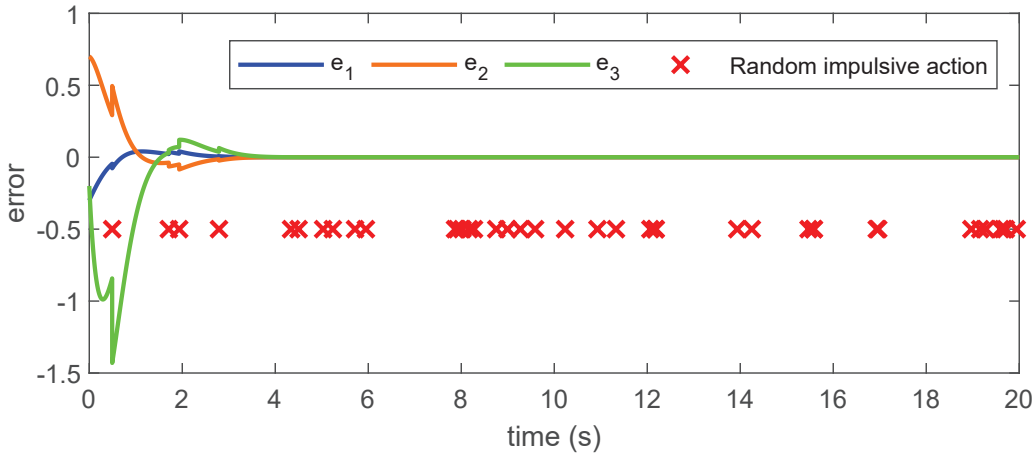

Figure 6. Error system of the hydraulic support pushing system with step signal.

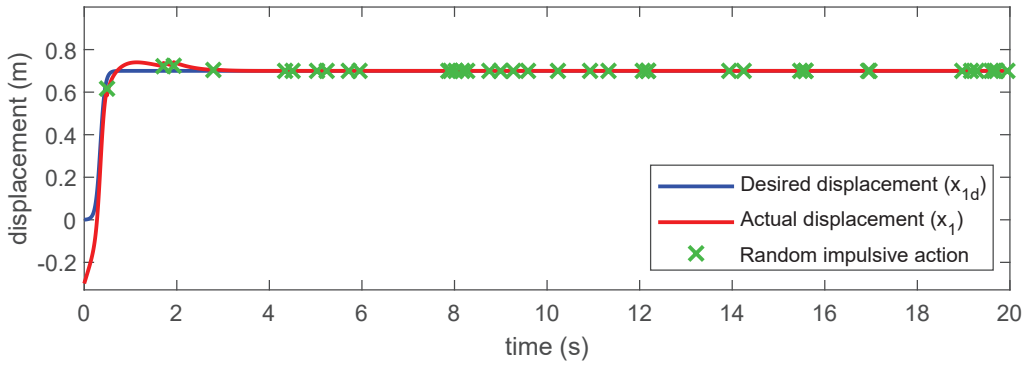

Figure 7. Comparison between the desired displacement and the actual displacement of the step signal with $C = 2$.

In the second simulation, a sinusoidal signal with an amplitude of 0.7 m and a frequency of 0.2 Hz is input into the system. Assume that the desired trajectories are $x_{1d}(t) = 0.7\sin(t)$, $x_{2d}(t) = 0.7\cos(t)$, $x_{3d}(t) = -0.7\sin(t)$, as shown by blue curve in Figure 8. In this simulation, we suppose that the intensity of the random impulses is $\beta = 2$ and the frequency of the random impulses is $\lambda = 1.5$. By applying Theorem 1, if we take control gain $C = 2.5$ and initial values $[x_{1d}(0), x_{2d}(0), x_{3d}(0)]^T = [0, 0.7, 0]^T$ and $[x_1(0), x_2(0), x_3(0)]^T = [0.3, 0, 0.2]^T$, then the actual trajectories can also track the desired trajectories under the random impulsive disturbances. The comparison and error curves of the desired output displacement and actual output displacement of the sinusoidal signal with random impulsive disturbances are shown in Figures 8 and 9. As counterexamples, Figure 10a and 10b illustrate the error performance of two classical and *unmodified* controllers, namely proportional-integral-derivative (PID) and sliding mode control (SMC), under the same random impulsive disturbances considered in this paper. The blue curves represent the actual system output trajectories, and the red crosses mark the occurrence instants of impulsive disturbances. For the PID controller with $u_{\text{iPID}}(t) = K_p e_i(t) + K_i \int_0^t e_i(\tau)d\tau + K_d \frac{de_i(t)}{dt}$, where gains are chosen as constants, although the parameters are tuned to achieve satisfactory performance under nominal conditions, the tracking error diverges gradually after several impulsive jumps. This is because the PID structure lacks an explicit mechanism to compensate for the sudden state resets caused by impulses, and the integral term may even accumulate the error, which leads to instability. For the SMC controller with surface $S(t) = c_1e_1(t) + c_2e_2(t) + e_3(t)$, the system is initially driven onto the sliding surface. However, each impulsive disturbance forces the state to abruptly leave the sliding surface, and the subsequent switching control cannot restore the sliding motion effectively under repeated random impulses. As a result, the error system eventually diverges. Both examples highlight the necessity of incorporating impulse statistics into the controller design, which is the key advantage of the proposed backstepping method.

Remark 4. Input-to-state (ISS)-based approaches mainly guarantee boundedness of the system state with respect to disturbance inputs, and the tracking error usually converges to an ultimate bounded set determined by the disturbance magnitude. Therefore, under persistent random impulsive disturbances, a residual tracking error may remain. In contrast, the proposed method establishes 2-ES sense, which provides an explicit convergence rate and faster attenuation of the tracking error after disturbances occur. This property is especially valuable for hydraulic servo systems that require high positioning precision and rapid recovery performance. Figure 11 illustrates the typical tracking performance of

the ISS-based controller in [34]. The blue curve is the desired trajectory, and the red curve is the actual output. The actual trajectory remains bounded but does not converge exactly to the reference, persistently staying within a residual error set whose size depends on the disturbance magnitude. This behavior is inherent to ISS-based methods, which only guarantee ultimate boundedness rather than exponential convergence. In comparison, the proposed method achieves 2-ES, which leads to complete convergence of the tracking error to zero and much faster recovery after impulsive events, as shown in Figure 8.

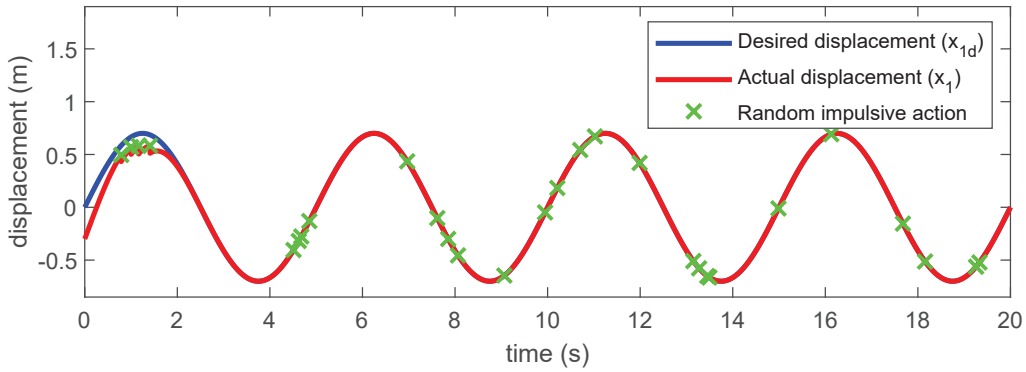

Figure 8. Comparison between the desired displacement and the actual displacement of the sinusoidal signal through the exponential manner.

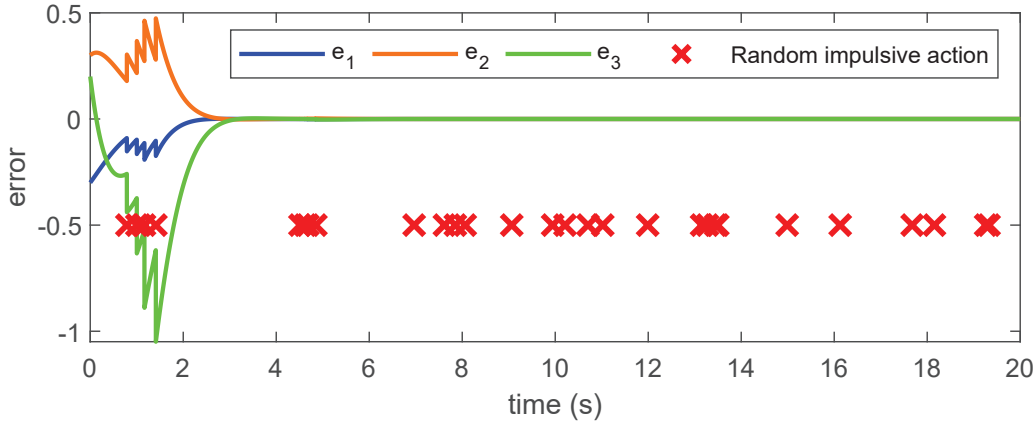

Figure 9. Error system of the hydraulic support pushing system with sinusoidal signal.

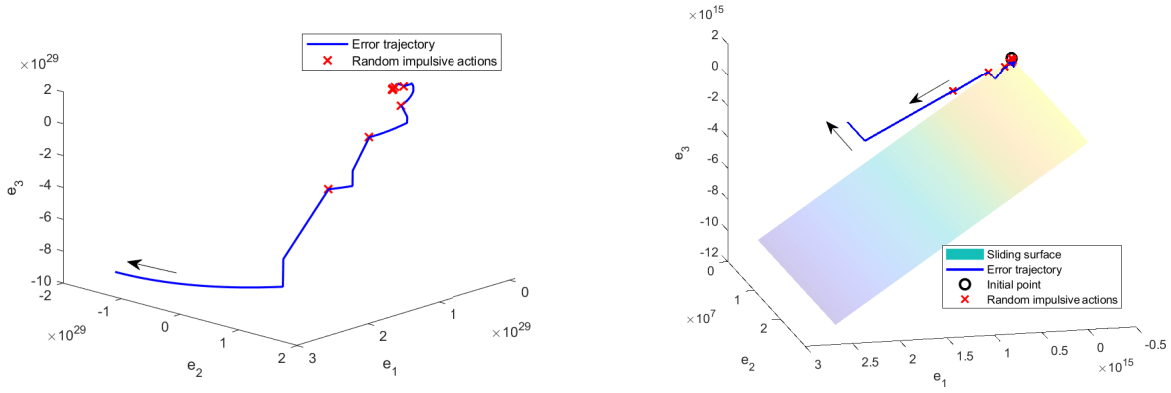

(a). PID method. **(b).** SMC method.

Figure 10. Error trajectories under two classical methods without considering impulsive disturbances. (a). Under PID controller. (b). Under SMC controller.

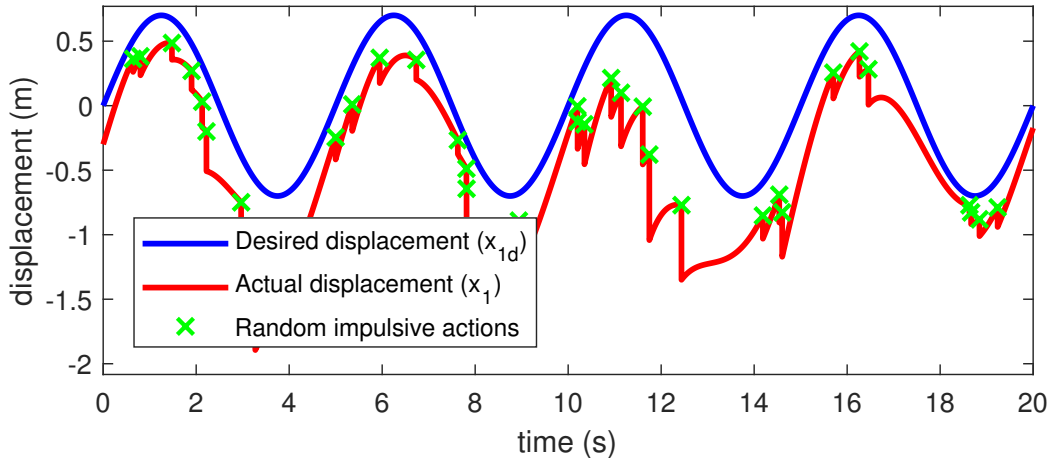

Figure 11. Comparison between the desired displacement and the actual displacement of the sinusoidal signal through the ISS manner.

5. Conclusions

This paper presented the mathematical model of the hydraulic support pushing system for the automation of hydraulic support coal mining technology. Based on the Lyapunov backstepping method and random analysis technique, we designed a controller for the hydraulic support pushing system against random impulsive disturbances, which enables the actual trajectories to track the desired trajectories. Moreover, a relationship among the continuous dynamics, impulsive intensity, and random impulsive sequences of the hydraulic support was established, which effectively improved the robustness of the hydraulic support pushing system. Nevertheless, one limitation of the current work is that the controller design is based on a linearized model, which may introduce certain bias when the system operates far from the equilibrium point or under severe nonlinear effects. Future work will focus on two aspects. First, we will refine the nonlinear modeling of the hydraulic support pushing system, incorporating friction, oil compressibility nonlinearities, and flow-pressure coupling, and extend the

stability analysis to the original nonlinear model under random impulsive disturbances. Second, an optimal gain selection strategy will be developed to balance convergence rate, control effort, and actuator constraints, thereby facilitating more systematic and practical controller tuning.

Author contributions

Mingzhong Li and Yuhao Qi: Methodology, formal analysis, investigation, resources, and writing-original draft preparation; Wei Wang, Qing Liu, and Shuai Liu: Conceptualization, software, validation, writing-original draft preparation; Yongming Li, Zhen Fu: Writing-review, editing, and supervision.

Use of AI tools declaration

The authors declare that they have not used Artificial Intelligence (AI) tools in the creation of this article.

Acknowledgment

This research was funded by National Key Research and Development Program of China under Grant 2023YFC2907504.

Conflict of interest

All authors declare no conflicts of interest in this paper.

References

1. C. Liu, H. Wang, B. Xiao, J. Nie, M. Liu, Initial commissioning parameters research of full-tailings backfill system in metal mine: From laboratory tests to industrial operation, *Constr. Build. Mater.*, **472** (2025), 140811. https://doi.org/10.1016/j.conbuildmat.2025.140811
2. J. Guo, Z. Wang, G. Feng, J. Bai, X. Wen, W. Huang, et al., Nonlinear mechanical analysis of load-bearing characteristics of coal-support-backfill system crossing abandoned roadways, *J. Rock Mech. Geotech.*, **18** (2025), 246–264. https://doi.org/10.1016/j.jrmge.2025.02.020
3. G. Yan, T. Zhang, X. Liu, C. Yao, C. Ai, The ADRC strategy research of electro-hydraulic servo pump control system based on dynamic load torque compensation for high-performance force control, *Int. J. Elec. Power*, **171** (2025), 110991. https://doi.org/10.1016/j.ijepes.2025.110991
4. V. Djordjevic, L. Dubonjic, M. Morato, D. Prsic, V. Stojanovic, Sensor fault estimation for hydraulic servo actuator based on sliding mode observer, *Math. Model. Control*, **2** (2022), 34–43. https://scidar.kg.ac.rs/handle/123456789/18601
5. M. Liang, D. Zheng, X. Fang, K. Li, C. Gu, G. Wu, et al., Research on attitude monitoring and decision-making of hydraulic support based on FBG sensor and BP neural network, *Opt. Fiber Technol.*, **93** (2025), 104219. https://doi.org/10.1016/j.yofte.2025.104219

6. V. Milic, Z. Situm, M. Essert, Robust position control synthesis of an electro-hydraulic servo system, *ISA Trans.*, **49** (2010), 535–542. https://doi.org/10.1016/j.isatra.2010.06.004
7. L. Liu, M. Liu, L. Wang, Q. Li, N. S. Ahmad, Design and implementation of a reference model-based disturbance observer for position control of electro-hydraulic Servo systems, *IEEE Access*, **13** (2025), 100530–100545. https://doi.org/10.1109/ACCESS.2025.3577656
8. A. Akers, M. Gassman, R. Smith, Hydraulic power system analysis, *Taylor Francis Group*, (2006). https://doi.org/10.1201/9781420014587
9. N. D. Manring, R. C. Fales, Hydraulic control systems, *John Wiley Sons*, (2019). https://doi.org/10.1002/9781119418528
10. Y. Zhang, H. Zhang, K. Gao, W. Xu, Q. Zeng, New method and experiment for detecting relative position and posture of the hydraulic support, *IEEE Access*, **7** (2019), 181842–181854. http://dx.doi.org/10.1109/ACCESS.2019.2958981
11. V. Stojanovic, Fault-tolerant control of a hydraulic servo actuator via adaptive dynamic programming, *Math. Model. Control*, **3** (2023), 181–191. https://www.aimspress.com/article/doi/10.3934/mmc.2023016
12. P. Zheng, J. Gao, Damping force and energy recovery analysis of regenerative hydraulic electric suspension system under road excitation: Modelling and numerical simulation, *Math. Biosci. Eng.* , **6** (2019), 6298–6318. http://dx.doi.org/10.3934/mbe.2019314
13. C. Sun, S. Chen, Z. Deng, Sliding mode control of electro-hydraulic servo based on neural network adaptive observer, *Electron. Res. Arch.*, **33** (2025), 6700–6719. http://dx.doi.org/10.3934/era.2025296
14. G. Zhuang, Y. Liu, X. Xie, J. Xia, H_∞ adaptive sliding-mode control for nonlinear delayed singular systems under impulsive attacks via piecewise auxiliary functions method, *IEEE T. Syst. Man Cy-S.*, **54** (2024), 5488–5500, https://doi.org/10.1109/TSMC.2024.3406523
15. X. Yu, Y. Hua, Y. Lu, Observer-based robust preview tracking control for a class of continuous-time Lipschitz nonlinear systems, *AIMS Math.*, **9** (2024), 26741–26764. http://dx.doi.org/10.3934/math.20241301
16. G. Zhuang, S. Xu, J. Xia, Q. Ma, Double feedback control-based H_∞ admissibilization for hybrid descriptor systems subject to external impulses and fast varying delays, *Syst. Control Lett.*, **184** (2024), 105719. https://doi.org/10.1016/j.sysconle.2024.105719
17. Q. Li, K. Zhang, H. Wei, F. Sun, J. Wang, Non-fragile asynchronous H_∞ estimation for piecewise-homogeneous Markovian jumping neural networks with partly available transition rates: A dynamic event-triggered scheme, *Neurocomputing*, **640** (2025), 130292. https://doi.org/10.1016/j.neucom.2025.130292
18. C. Wang, J. Wang, Q. Guo, Z. Liu, C. L. P. Chen, Disturbance observer-based fixed-time event-triggered control for networked electro-hydraulic systems with input saturation, *IEEE T. Ind. Electron.*, **72** (2025), 1784–1794. http://doi.org/ 10.1109/TIE.2024.3429638
19. L. Wan, X. Wu, C. Wang, X. Zhang, Mechanical-hydraulic integration modeling and simulation of hydraulic support, *2010 International Conference on Computer Application and System Modeling (ICCASM 2010)*, (2010). http://dx.doi.org/10.1109/ICCASM.2010.5619349

20. H. Liu, J. Liu, Data collecting and processing system of hydraulic support model test, *2011 International Conference on Electric Information and Control Engineering*, (2011), 1266–1268. http://dx.doi.org/10.1109/ICEICE.2011.5777959

21. L. Zhang, L. Zhao, Y. Qian, H. Xiao M. Luo, A Multi-Segment Pushing Curve Synchronous Control System for Hydraulic Support, *2019 IEEE 3rd Advanced Information Management, Communicates, Electronic and Automation Control Conference (IMCEC)*, (2019), 458-464. http://dx.doi.org/10.1109/IMCEC46724.2019.8984188

22. T. Hou, Z. Kou, J. Wu, B. Zhang, Y. Peng, Research on positioning control strategy of hydraulic support pushing system based on multistage speed control valve, *Sci-Rep.*, **14** (2024), 19046. https://doi.org/10.1038/s41598-024-70087-1

23. Z. Zhang, Y. Liu, L. Bo, Y. Wang, Enhanced path tracking control of hydraulic support pushing mechanism via adaptive sliding mode technique in coal mine backfill operations, *Heliyon*, **10** (2024), e38437. https://doi.org/10.1016/j.heliyon.2024.e38437

24. L. Li, Y. Huang, J. Tao, C. Liu, K. Li, Featured temporal segmentation method and AdaBoost-BP detector for internal leakage evaluation of a hydraulic cylinder, *Measurement*, **130** (2018), 279–289. https://doi.org/10.1016/j.measurement.2018.08.029

25. X. Ren, Q. Guo, T. Li, Initial condition-free prescribed performance fault-tolerant control of electro-hydraulic servo systems with state constraints, *Nonlinear Dyn.*, **113** (2025), 11723–11743. https://doi.org/10.1007/s11071-024-10804-7

26. W. H. Chen, H. Xiang, Composite anti-disturbance impulsive control for a class of nonlinear systems via disturbance observers, *Nonlinear Anal-Hybri.*, **57** (2025), 101599. https://doi.org/10.1016/j.nahs.2025.101599

27. Y. Wang, C. Li, H. Wu, H. Deng, Stabilization of nonlinear delayed systems subject to impulsive disturbance via aperiodic intermittent control, *J. Franklin I.*, **361** (2024), 106675. https://doi.org/10.1016/j.jfranklin.2024.106675

28. N. Zhao, Y. Qiao, Stability analysis of Clifford-valued memristor-based neural networks with impulsive disturbances and its application to image encryption, *Appl. Math. Comput.*, **475** (2024), 128710. https://doi.org/10.1016/j.amc.2024.128710

29. Z. Ni, C. Wu, S. Wu, Identification of time-varying inertia tensor parameters of a space solar power satellite based on a robust weighted recursive algorithm under impulsive disturbance, *Aerosp. Sci. Technol.*, **144** (2024), 7108796. https://doi.org/10.1016/j.ast.2023.108796

30. R. Zhou, Z. Tu, Q. Liu, Y. Wang, X. Liu, Asymptotic feedback stabilization of Boolean control networks with random impulsive disturbances, *IEEE T. Cybernetics*, **55** (2025), 1–12. http://dx.doi.org/10.1109/TCYB.2025.3589571

31. H. Wang, G. Wei, S. Wen, T. Huang, Impulsive disturbance on stability analysis of delayed quaternion-valued neural networks, *Appl. Math. Comput.*, **390** (2021), 125680. https://doi.org/10.1016/j.amc.2020.125680

32. C. Liu, T. Wei, X. He, X. Li, Sliding-mode control for target tracking of omnidirectional mobile robots subject to impulsive deception attacks, *Chaos, Soliton. Fract.*, **187** (2024), 115439. https://doi.org/10.1016/j.chaos.2024.115439

33. W. He, F. Qian, Q. L. Han, G. Chen, Almost sure stability of nonlinear systems under random and impulsive sequential attacks, *IEEE T. Automat. Contr.*, **65** (2020), 3879–3886. http://dx.doi.org/10.1109/TAC.2020.2972220

34. W. Li, M. Li, J. Liu, G. Wang, Y. Qi, W. Wang, et al., Input-to-state stability of the electro-hydraulic servo system with a backstepping-based impulsive correction control, *AIMS Math.*, **10** (2025), 30927-30941. http://dx.doi.org/10.3934/math.20251357

AIMS Press